CONF-961001--2

A SIMPLE MODEL FOR CYCLIC VARIATIONS IN A SPARK-IGNITION ENGINE

C. S. Daw
J. B. Green, Jr.
M. B. Kennel
J. F. Thomas
Oak Ridge National Laboratory
Oak Ridge, Tennessee 37831-8088

C. E. A. Finney
The University of Tennessee
Knoxville, Tennessee 37996-2210

F. T. Connolly
Ford Motor Company
Dearborn, Michigan 48121-2053

RECEIVED
OCT 29 1996
OSTI

Prepared by the
OAK RIDGE NATIONAL LABORATORY
Oak Ridge, Tennessee 37831

managed by
LOCKHEED MARTIN ENERGY RESEARCH CORP.
for the
U.S. DEPARTMENT OF ENERGY
under Contract No. DE-AC05-96OR22464.

MASTER

The submitted manuscript has been authored by a contractor of the U.S. Government under contract No. DE-AC05-96OR22464. Accordingly, the U.S. Government retains a nonexclusive, royalty-free license to publish or reproduce the published form of this contribution, or allow others to do so, for U.S. Government purposes.

DISTRIBUTION OF THIS DOCUMENT IS UNLIMITED

DISCLAIMER

Portions of this document may be illegible in electronic image products. Images are produced from the best available original document.

A simple model for cyclic variations in a spark-ignition engine

C.S. Daw[†], C.E.A. Finney[‡], J.B. Green, Jr.[†], M.B. Kennel[†], J.F. Thomas[†]
[†] Oak Ridge National Laboratory, Oak Ridge, Tennessee 37831-8088
[‡] University of Tennessee, Knoxville, Tennessee 37996-2210

F.T. Connolly
Ford Motor Company, Dearborn, Michigan 48121-2053

ABSTRACT

We propose a simple, physically oriented model that explains important characteristics of cyclic combustion variations in spark-ignited engines. A key model feature is the interaction between stochastic, small-scale fluctuations in engine parameters and nonlinear deterministic coupling between successive engine cycles. Prior-cycle effects are produced by residual cylinder gas which alters volume-average in-cylinder equivalence ratio and subsequent combustion efficiency. The model's simplicity allows rapid simulation of thousands of engine cycles, permitting in-depth statistical studies of cyclic variation patterns. Additional mechanisms for stochastic and prior-cycle effects can be added to evaluate their impact on overall engine performance. We find good agreement with our experimental data.

INTRODUCTION

Ever since the investigations of Clerk [1], researchers have reported apparently conflicting observations of cyclic combustion variations in spark-ignition engines. With increasing emphasis on lean fueling and exhaust gas recirculation to minimize NO_xemissions, cyclic variability (CV), also known as cyclic dispersion, has received renewed attention. Examples of this recent interest can be found in [2 – 12]. In most studies, CV has been described as either stochastic (random) or deterministic in nature [10 – 12]. Furthermore, any determinism has been typically characterized in strictly linear terms (e.g., cycle-to-cycle autocorrelation functions).

We propose a model that combines both stochastic and nonlinear deterministic elements. We avoid complex spatial details, instead focusing on the global combustion process and how that process evolves under the combined influence of stochastic and deterministic processes over thousands of engine cycles. Our objective is to produce a simple model that produces dynamical CV patterns similar to a real engine. In addition to dynamic similarity, we intend our model to be physically realistic so that it correctly predicts CV trends with as-fed fuel-air ratio and provides fundamental insight into the effect of the key processes.

MODEL DEVELOPMENT

Our model is structured around the interaction between deterministic and stochastic processes. We assume that the primary deterministic aspect of CV arises from the presence of retained fuel and oxidizer from one cycle to the next. We further assume that the main stochastic element is modeled as random fluctuations in one or more of the key deterministic parameters such as injected fuel-to-air ratio, residual fraction, and the lower ignition limit. In principle, all of these parameters can undergo effectively random perturbations due to complex processes such as in-cylinder turbulence, fuel-droplet vaporization, and wall deposits.

The model is discrete in time, representing each full cycle (including intake and exhaust) as a single event. We first present the model in dimensional quantities and then normalize it to be nondimensional. The dynamical variables which define the two-dimensional state space are the masses of air and fuel present in the cylinder at the time of spark.

INTAKE PHASE – Total mass is residual mass from the previous cycle plus new intake:

$$m[n] = m_{\rm res}[n] + m_{\rm new}[n] \quad (1)$$

$$a[n] = a_{\rm res}[n] + a_{\rm new}[n] \quad (2)$$

The quantities $m[n]$ and $a[n]$ are the mass of fuel and air in the cylinder immediately preceding spark, and $m_{\rm res}[n]$ and $a_{\rm res}[n]$ are the masses of unreacted air and fuel remaining from the previous cycle. Our model currently ignores the inert combustion products, although these can be easily added. The new mass fed to the cylinder is inferred from two algebraic relationships. First,

$$\frac{m_{\rm new}[n]R}{a_{\rm new}[n]} = \phi_o(1 + \sigma_\phi N(0,1)) \quad (3)$$

Eq. 3 reflects that the injected fuel-air ratio is assumed to have a mean value ϕ_o (i.e., the mean equivalence ratio) and a Gaussian distribution with standard deviation σ_ϕ. Physically, the fluctuations in ϕ arise from vaporization or turbulence effects, and our model simulates the fluctuations using a new random number for each cycle. The parameter R gives the ratio of air to fuel mass

at stoichiometric burning, so that $\phi_o = 1$ is the nominally stoichiometric fuel condition. The value of R depends only on the fuel composition, assumed constant in our model (e.g., 14.6). A second constraint on fuel and air injection is

$$\frac{m[n]}{w_f} + \frac{a[n]}{w_a} = M \tag{4}$$

Eq. 4 satisfies the restriction that the total molar content of the in-cylinder fuel-air mixture is constant. Stated simply, the amounts of new fuel and air that can be added to the cylinder must be reduced in proportion to the amount of residual gas retained from the previous cycle. This constraint can be reasonably justified assuming constant input pressure and temperature and an ideal-gas approximation. w_f and w_a are the average molecular weights of fuel and air. In our simulations, we use $w_f = 114\,\mathrm{g/mol}$ and $w_a = 29\,\mathrm{g/mol}$. Eq. 3 and 4 are used together to define the amount of new fuel and air injected into the cylinder each cycle.

COMBUSTION EFFICIENCY – We model the net efficiency of combustion C as a function only of the in-cylinder fuel-to-air ratio $\Phi[n] = Rm[n]/a[n]$ at the time of spark:

$$C[n] = C(\Phi[n]) \tag{5}$$

The exact functional form of the combustion efficiency is another somewhat arbitrary external parameter, but its general shape is governed by physics. Specifically, we mean here that it is generally observed that the lean combustion limit is relatively sharp [13]; that is, as equivalence ratio is reduced from above the critical to below, combustion rapidly declines from nearly complete to none. Such a sharp drop in engine combustion efficiency is indicated by results such as those reported in [14]. For hydrocarbon fuels, the critical equivalence ratio is typically about 0.5–0.6 [13]. The steepness of this curve can be explained in terms of the flame-front propagation and its sensitivity to small changes in heat-release rate near the lean limit [13].

The particular choice of an exponential sigmoidal function to interpolate between these physically determined limits is arbitrary, but the dynamical patterns one sees with alternate functional forms are nearly identical, as long as the essential physical features are present: a plateau starting at stoichiometric conditions with a sharp drop-off upon approaching the lean limit. For $\Phi \geq 1$, combustion is fuel rich and is limited by the amount of air:

$$C(\Phi) = \frac{C_{\max}}{\Phi} \tag{6}$$

The consideration of very fuel-rich conditions is included only for completeness; the dynamical system almost never attains such conditions in the situations we consider. For $\Phi < 1$, combustion is fuel lean. For ease of understanding, the position of the knee is parameterized by ϕ_l and ϕ_u, the conditions where the efficiency is approximately 10 and 90 percent of the maximum, respectively. Then, given $\phi_m = (\phi_l + \phi_u)/2$,

$$C(\Phi) = \frac{C_{\max}}{1 + 100^{-\frac{\Phi - \phi_m}{\phi_u - \phi_l}}} \tag{7}$$

The function in Eq. 7 gives a smooth curve taking on values from 0 to $C_{\max}$ with a knee centered at ϕ_m and provides the essential nonlinearity in the dynamics. Figure 1 shows the function shape defined by Eq. 6 and 7.

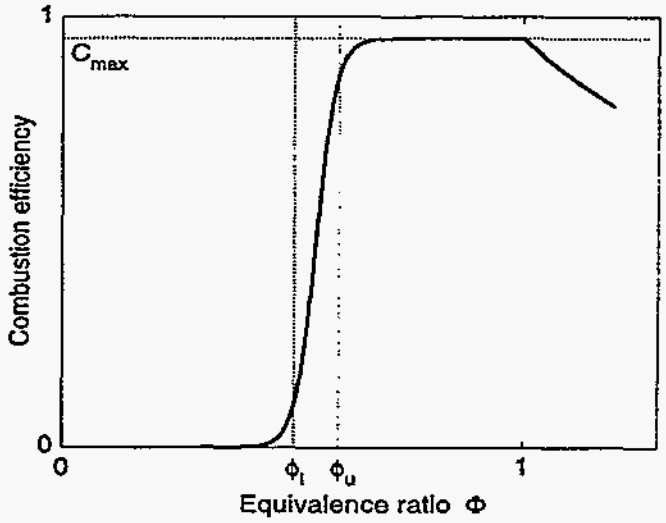

Figure 1: Combustion-efficiency function assumed to account for residual-gas effects. Based on typical lean-limit measurements, ϕ_m is expected to be between 0.5 to 0.6.

COMBUSTION AND EXHAUST PHASE – The heat released in the combustion cycle (the primary experimental measurement) is proportional to $Q[n] = C[n]m[n]$. The principal physical mechanism for cycle-to-cycle coupling is that a certain fraction F of the unreacted air and fuel remains in the cylinder for the next cycle, thus altering the next cycle's charge. The remaining fuel is F times the fuel not combusted:

$$m_{\mathrm{res}}[n+1] = Fm[n](1 - C[n]) \tag{8}$$

and the remaining air is that not used in the reaction,

$$a_{\mathrm{res}}[n+1] = F(a[n] - RC[n]m[n]) \tag{9}$$

We model fluctuations in F by letting it vary each cycle by a random number:

$$F = F_o(1 + \sigma_F N(0,1)) \tag{10}$$

As with ϕ, Eq. 10 reflects that we allow F to vary about its nominal mean value F_o as a Gaussian process with standard deviation σ_F. Experimental measurements suggest that values of F_o can vary from 0 to 0.3 depending on engine design and operating conditions [14].

NONDIMENSIONALIZATION – It is often convenient to nondimensionalize dynamical maps of this type. Specifically, fuel masses and air masses will be measured in units of what the fuel and air mass (denoted m_o and a_o) would be at perfectly combusting stoichiometric conditions with no residuals ($C = 1$, $m_{\mathrm{res}} = a_{\mathrm{res}} = 0$): Given $Rm_o = a_o$ and the gas-law equation, we can solve

$$m_o = \frac{M}{\frac{1}{w_f} + \frac{R}{w_a}} \tag{11}$$

$$a_o = Rm_o \tag{12}$$

We now define dimensionless fuel (m^*, m^*_{res}, m^*_{new}) and air (a^*, a^*_{res}, a^*_{new}) masses by normalizing the appropriate quantities with m_o and a_o, respectively. Note that the variables C, ϕ_o, Φ, F and R are already dimensionless.

MODEL SUMMARY – Defining $\Sigma = w_f/w_a$, the ratio of the molecular weights, we summarize the nondimensionalized model equations. For the intake process,

$$m^*[n] = m^*_{res}[n] + m^*_{new}[n] \quad (13)$$

$$a^*[n] = a^*_{res}[n] + a^*_{new}[n] \quad (14)$$

$$\frac{m^*[n] + \Sigma R a^*[n]}{1 + \Sigma R} = 1 \quad (15)$$

$$\frac{m^*_{new}[n]}{a^*_{new}[n]} = \phi_o(1 + \sigma_\phi N(0,1)) \quad (16)$$

For the combustion process,

$$\Phi[n] = \frac{m^*[n]}{a^*[n]} \quad (17)$$

$$C[n] = C(\Phi[n]) \quad (18)$$

$$Q^*[n] = C[n]m^*[n] \quad (19)$$

For the exhaust process,

$$F = F_o(1 + \sigma_F N(0,1)) \quad (20)$$

$$m^*_{res}[n+1] = F(1 - C[n])\, m^*[n] \quad (21)$$

$$a^*_{res}[n+1] = F(a^*[n] - C[n]m^*[n]) \quad (22)$$

When intake, combustion and exhaust processes are combined,

$$m^*[n+1] = F(1 - C[n])\, m^*[n] + m^*_{new}[n] \quad (23)$$

$$a^*[n+1] = F(a^*[n] - C[n]Rm^*[n]) + a^*_{new}[n] \quad (24)$$

The overall model is thus characterized as a two-dimensional dynamic map, taking the state variables m^* and a^* one cycle forward in time:

$$m^*[n+1] = A[m^*[n], a^*[n], \phi_o, \sigma_\phi, F_o, \ldots] \quad (25)$$

$$a^*[n+1] = B[m^*[n], a^*[n], \phi_o, \sigma_\phi, F_o, \ldots] \quad (26)$$

for mapping functions A and B. A crucial feature of this mapping is the nonlinearity produced by the sharp change in combustion efficiency with ϕ_o. Another important feature is that the random perturbations in Φ and F can augment the complexity produced by the nonlinear mapping. In effect, the nonlinearity amplifies stochastic perturbations.

In order to produce a mapping output that can be more directly compared with experimental observations, we look at the mapping of heat release from one cycle to the next:

$$Q^*[n+1] = f(Q^*[n]) \quad (27)$$

for mapping function f and Q^* defined in Eq. 19. A key theorem from nonlinear dynamics [15] holds that equivalent information about the dynamic patterns can be obtained by using just this single observable. Thus we consider the sequence of measured heat releases $Q^*[t], Q^*[t+1], \ldots, Q^*[t+n]$ as the principal model output.

The sequences of plots in Fig. 2–4 illustrate the effect of changes in ϕ_o and the model parameters. The parameter changes illustrated were selected to be within the expected ranges described earlier. Each plot is produced by iterating the mapping (Eq. 23 and 24) for a fixed ϕ_o and the indicated parameter values beginning with arbitrary initial values for m^* and a^*. Neglecting initial transients, the heat-release values for several hundred iterates are plotted, and then the process is repeated for a slightly different ϕ_o. The final result plotted over a range of ϕ_o is referred to as a *bifurcation diagram* and illustrates the expected trend in heat-release behavior for varying ϕ_o. See Moon [16] for a detailed explanation of bifurcation plots.

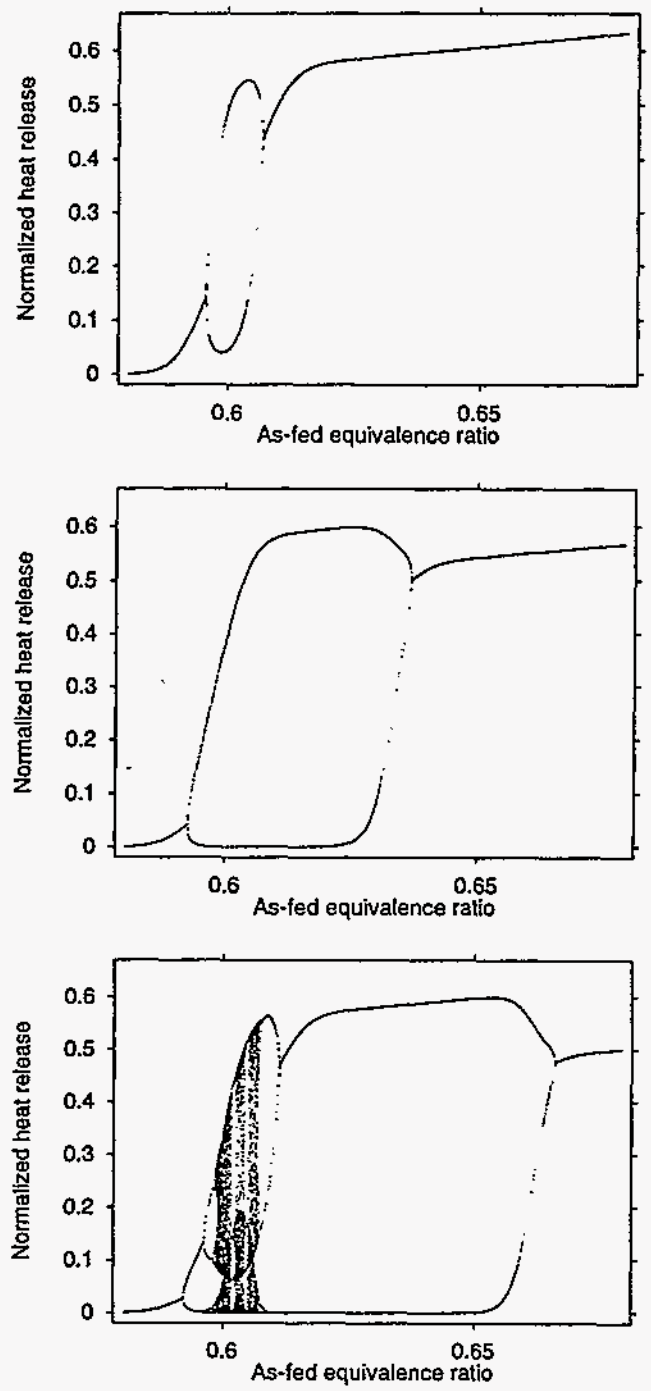

Figure 2: Model equivalence-ratio (ϕ_o) bifurcation plots with $F_o = 0.05$ (top), $F_o = 0.1$ (middle), and $F_o = 0.25$ (bottom). Fixed model parameters are $\sigma_\phi = \sigma_F = 0$, $\phi_l = 0.59$, and $\phi_u = 0.60$.

Although the bifurcation details change with parameter values, certain general trends are apparent:

- Near stoichiometric conditions, the amount of fuel burned in each cycle stabilizes to a single fixed value (a fixed point);

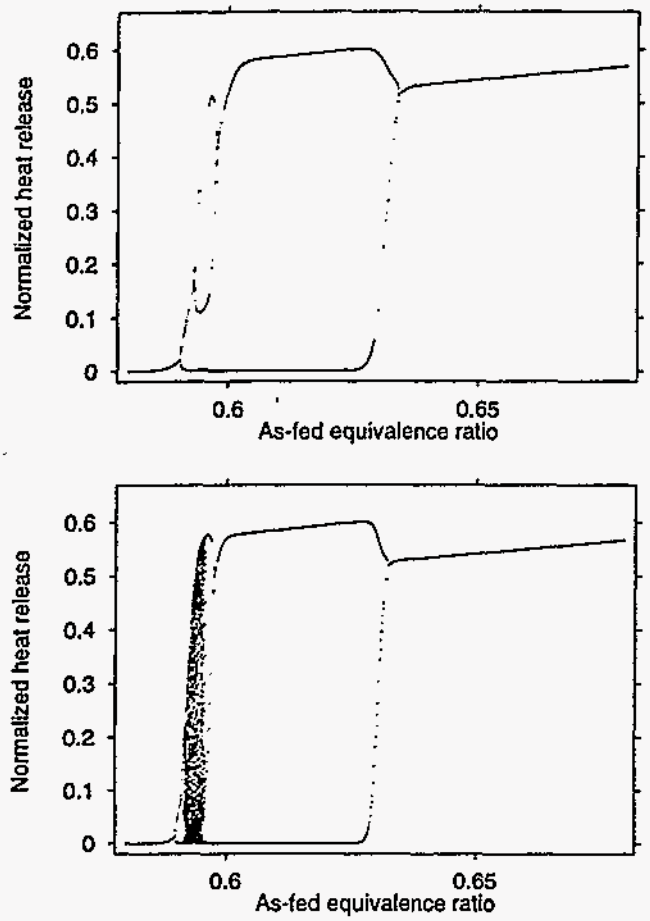

Figure 3: Model equivalence-ratio (ϕ_o) bifurcation plots with $\phi_l = 0.593$ (top) and $\phi_l = 0.595$ (bottom). Fixed model parameters are $\sigma_\phi = \sigma_F = 0$, $\phi_u = 0.595$, and $F_o = 0.15$

- For ϕ_o below a critical value, the amount of fuel burned oscillates between two distinct values (a period-2 bifurcation);
- For still lower ϕ_o, combustion oscillations become more complex, leading to multi-period or chaotic patterns;
- For ϕ_o below the lean limit, all combustion ceases;
- When stochastic perturbations (noise) are added to either ϕ or F or both, the detailed bifurcation structure becomes fuzzy but still reflects the underlying sequence of period-2 bifurcations and/or chaos;
- Noise also causes the initial bifurcation to occur at a higher ϕ_o (i.e., higher than when no noise is added) and maintains combustion in the extreme lean limit.

Briefly stated, the model predicts that combustion becomes unstable near the lean limit due to the onset of period-doubling bifurcations arising from deterministic processes. This instability is enhanced by random perturbations in parameters such as as-fed equivalence ratio and residual fraction. The prediction of a period-doubling instability is important because it provides a unique signature that can be experimentally verified and because it has been extensively studied in other systems [16].

EXPERIMENTAL DATA ACQUISITION

We collected experimental data from a production V8 engine with standard port fuel injection connected to a DC motoring dynamometer. Injected fuel-air ratio was decreased from stoichiometric to very lean (where the engine was producing little torque). The nominal operating condition was 1200 RPM, 27.1N·m brake torque, 20 degrees BTC spark. We operated the dynamometer in speed-control mode to keep the engine running at constant speed despite erratic combustion at very lean conditions. Feedback engine controllers were engaged to achieve an operating condition; once the condition was achieved, the feed-

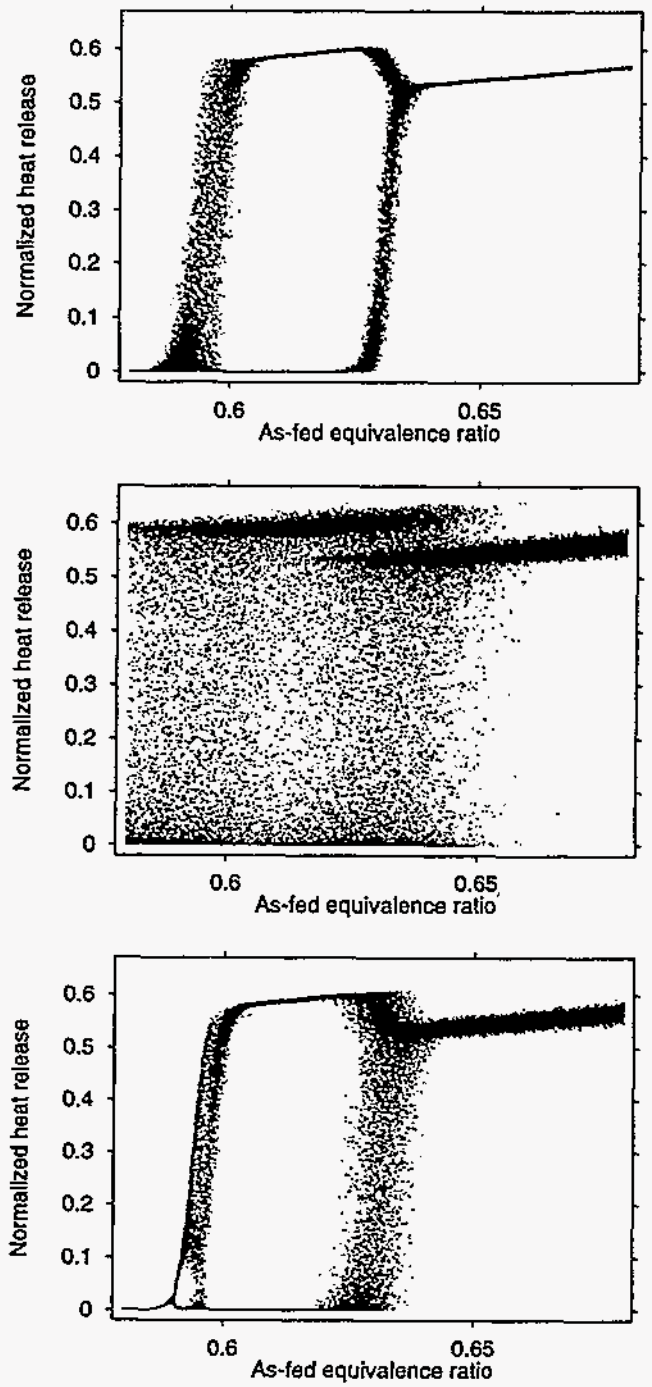

Figure 4: Model equivalence-ratio (ϕ_o) bifurcation plots with $\sigma_\phi = 0.001$ (top), $\sigma_\phi = 0.01$ (middle), and $\sigma_F = 0.01$ (bottom). Fixed model parameters are $\phi_l = 0.590$, $\phi_u = 0.595$, and $F_o = 0.15$.

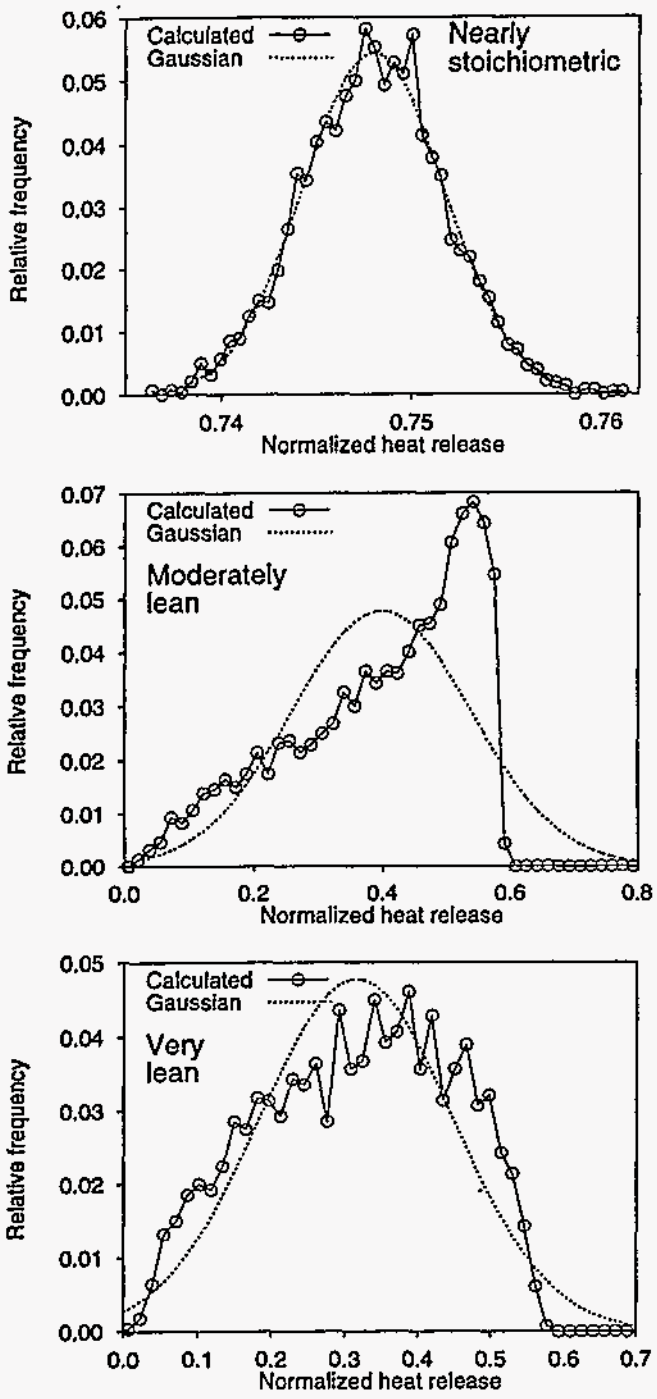

Figure 5: Model heat release frequency histograms for nearly stoichiometric (top), moderately lean (middle), and very lean (bottom) fueling. Dynamic noise is included by adding Gaussian noise to the as-injected fuel-air ratio.

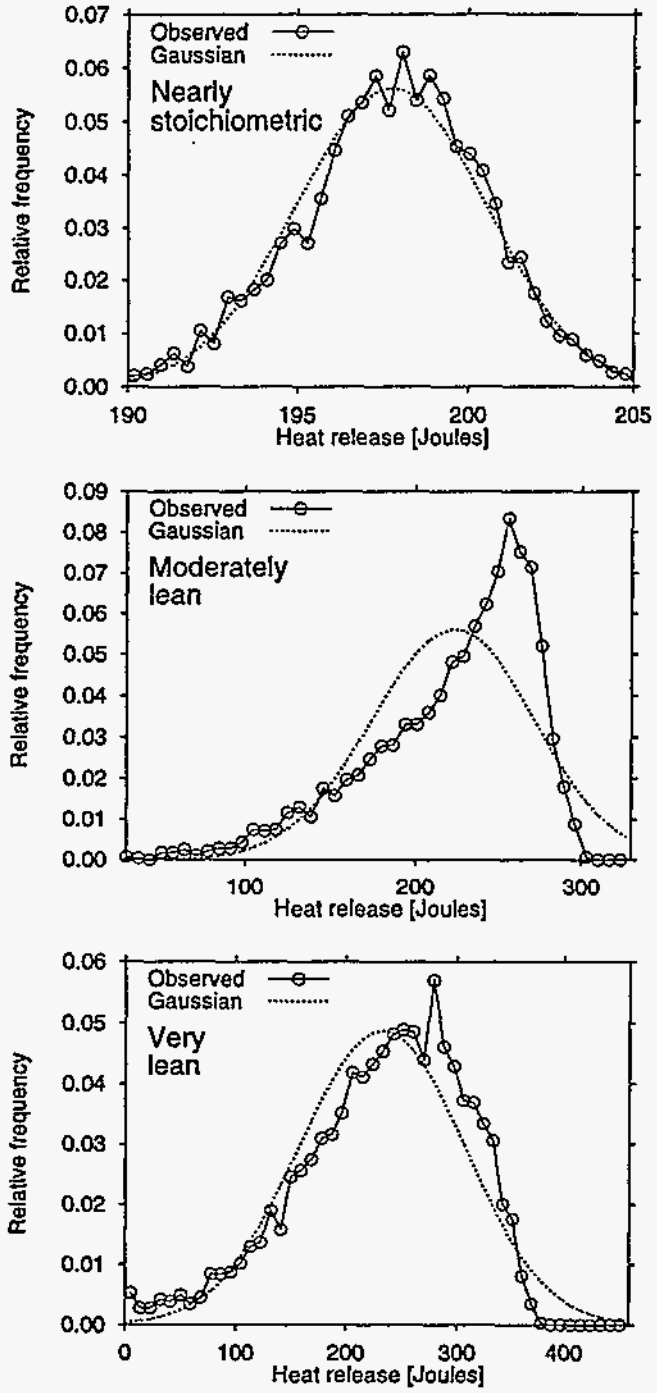

Figure 6: Experimental heat release frequency histograms for nearly stoichiometric (top), moderately lean (middle), and very lean fueling (bottom). Note similarity to Fig. 5.

back controllers were shut off, and the engine was run in open-loop mode, except for dynamometer speed control. This assured that combustion was minimally influenced by feedback controllers while the engine ran at constant speed. We recorded combustion pressure once per crank angle degree from a single cylinder and nominal operating conditions at a 50 Hz rate for over 2800 contiguous cycles. Cycle-by-cycle heat release was calculated by integrating the pressure data in a manner equivalent to the Rassweiler-Withrow method [14].

DISCUSSION

Ideally, it would be desirable to verify that our experimental engine produces bifurcation patterns such as those illustrated in Fig. 2–4. This verification is impractical, however, because of the large number of experiments required. Instead, we chose to use other techniques from nonlinear dynamics theory that permit comparison of a smaller number of experimental operating points with the model predictions. Our specific objective in this case was to compare the predicted and observed trends while the as-fed equivalence ratio is reduced from nearly stoi-

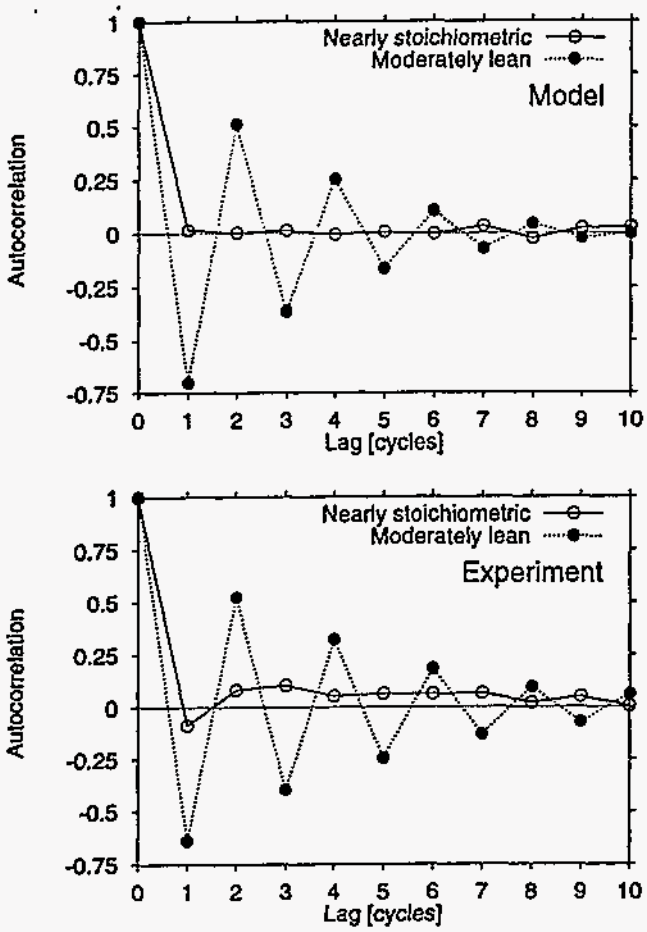

Figure 7: Autocorrelation functions for model (top) and experimental (bottom) for nearly stoichiometric and moderately lean fueling.

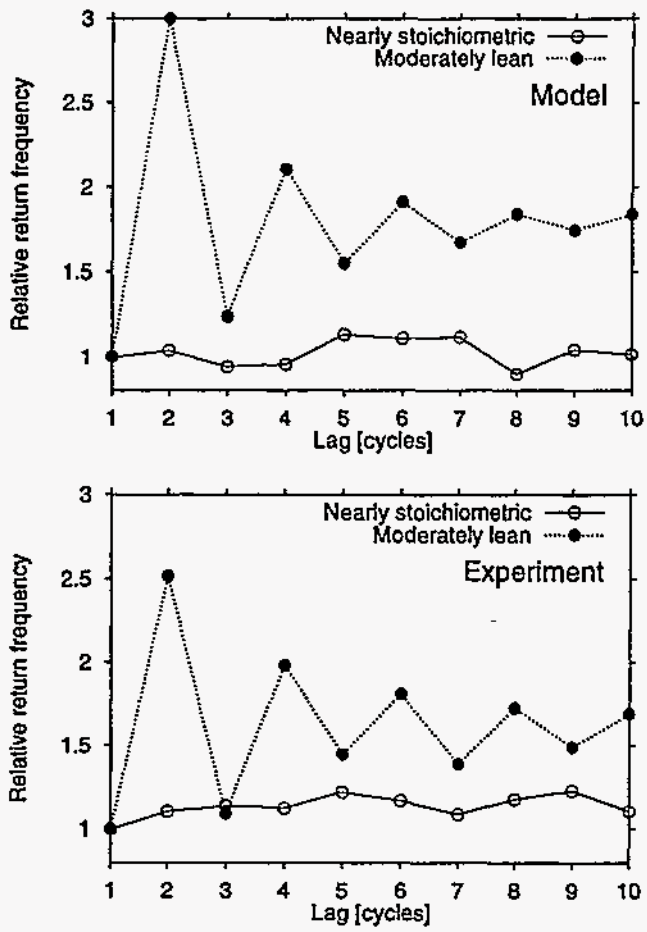

Figure 8: Relative return frequency plots for model (top) and experimental (bottom) for nearly stoichiometric and moderately lean fueling. A strong period-2 pattern in heat release develops for moderately lean fueling, as is seen in the peaks at multiples of 2-cycle lag. The observation of the periodicity at longer lags is increasingly obscured by the presence of noise.

chiometric to very lean. We did not intend to obtain exact "fits" of the model with the experiemental data but rather to look for evidence that the experiment exhibited a similar type of instability. In particular, we sought to determine if the observed CV patterns could be explained by period-doubling bifurcations that are enhanced by stochastic perturbations in engine parameters.

To establish the predicted trends in a format more comparable with our experiment, we ran the model at nearly stoichiometric, moderately lean, and very lean fueling conditions for parameter values we expect to be within realistic ranges. Output for each model condition consisted of heat-release values for 2800 consecutive cycles. Within the parameter ranges covered in Fig. 2 – 4, we found that the basic trends were similar. Thus we expected that at least qualitative similarities between the model and experimental data could be verified.

One of the simplest comparisons that can be made between the model and experiment is their heat-release probability histograms. While such histograms do not reflect dynamics, they do reflect the overall probability distributions that should be consistent if the model is correct. Figures 5 and 6 compare model and experimental heat-release frequency distributions for three fueling conditions. Gaussian distributions with the same mean and standard deviation are also depicted for each case for comparison. For both model and experiment, nearly stoichiometric fueling is characterized by simple Gaussian fluctuations in heat release, reflecting the dominance of stochastic processes. Decreasing ϕ leads to deviations from Gaussian structure, reflecting an increasing influence from residual-gas effects. In effect, the determinism nonlinearly transforms the Gaussian perturbations. The relative size of the input noise is no more than 2 percent, yet the size of the output fluctuations relative to the mean magnitude can be on the order of 50 to 100 percent in physically realistic conditions. We term this behavior *nonlinear noise amplification.*

Figure 7 illustrates similar model and experiment behavior using the autocorrelation function. Figure 7 suggests that a period-2 pattern has emerged at moderately lean fueling. The "hidden" period 2 is revealed by a significant autocorrelation value at multiple intervals of two. As in Fig. 2 – 4, the periodicity is "blurred", but the effect is present. No peaks are seen at nearly stoichiometric fueling, where bifurcation has not occurred.

We find that algorithms specifically developed for analyzing nonlinear time series data also reveal period-2 bifurcations. This is illustrated in Fig. 8, where is plotted a quantity we refer to as *relative return frequency* versus lag in combustion cycles. Relative return frequency reflects the likelihood that a combus-

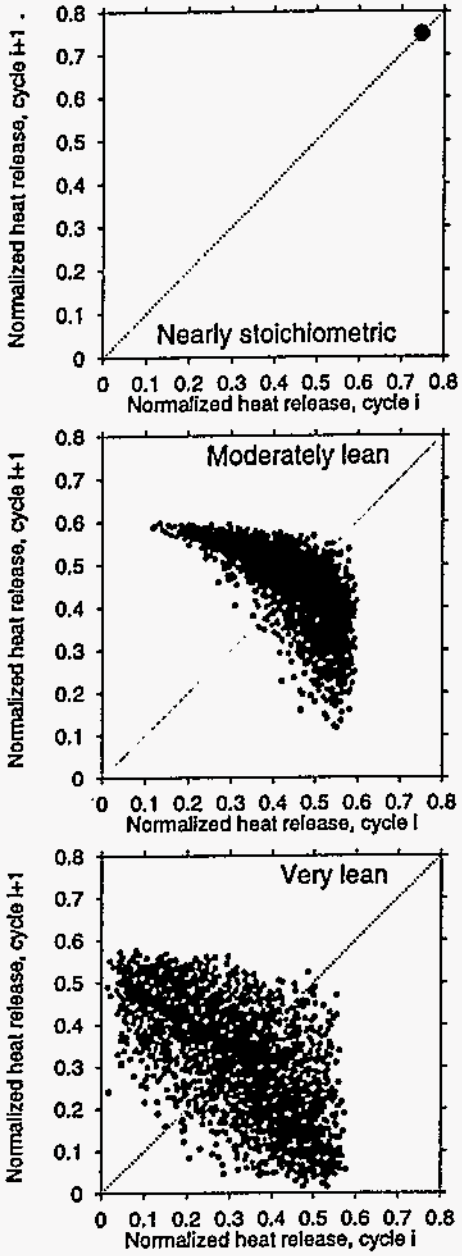

Figure 9: Model return map for nearly stoichiometric (top), moderately lean (middle), and very lean (bottom) fueling.

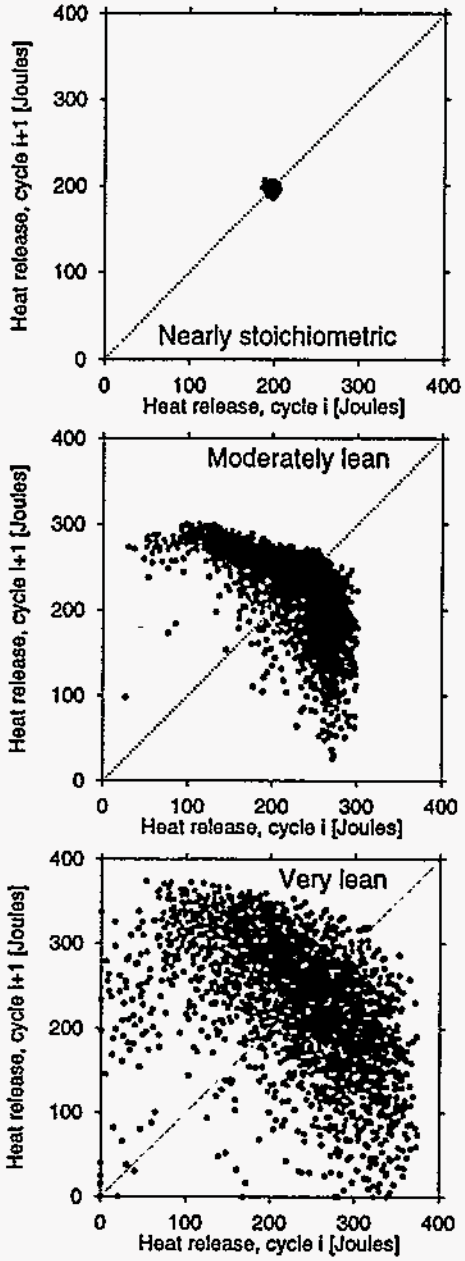

Figure 10: Experimental return maps for nearly stoichiometric (top), moderately lean (middle), and very lean (bottom) fueling.

tion event occurring after some specified number of cycles will be similar to the current combustion within some specified tolerance. In the figure, the tolerance is approximately 20 percent of the standard deviation in heat release over several thousand cycles. Thus, when two combustion events separated by one or more cycles are found to differ by no more than this tolerance, they are counted as repeat events. By comparing the relative frequency of repeat events for different numbers of intervening cycles, the presence of multiple periods can be detected (i.e., combustion sequences that repeat over some fixed number of cycles).

In the figure, the repeat frequency for each lag has been normalized with the repeat frequency for a lag of one cycle, hence the term "relative". At stoichiometric conditions, the likelihood of repeats is equal regardless of the number of intervening cycles. However, at moderately lean conditions, repeat combustion events are much more likely after cycle intervals that are multiples of two. This latter result thus reflects underlying period-2 patterns in both the model predictions and the experimental data. In general, linear techniques such as the autocorrelation function are not as good at elucidating the behavior of nonlinear and potentially chaotic dynamical systems as methods designed for this situation.

Another analytical method which reveals more information about nonlinear dynamic patterns is the *return map*. Figures 9 and 10 depict return-map sequences for the model and experiment at three similar fueling conditions. Each return map is constructed by plotting the heat release for cycle i versus the heat release for cycle $i+1$, where i is stepped sequentially through each time series. The resulting pattern reveals the relationship between the heat releases for successive cycles. For cycles that are completely uncorrelated, one expects to obtain an

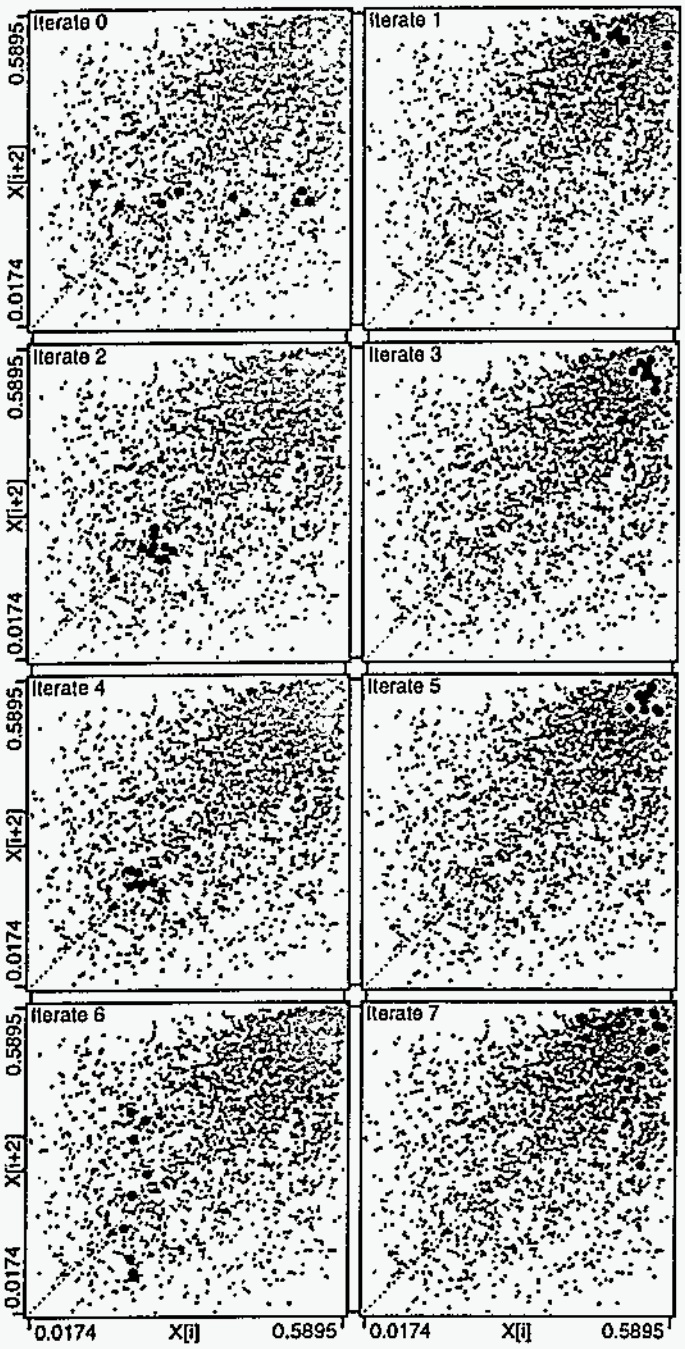

Figure 11: Model return map sequences for moderately lean fueling. Dark points represent uncorrelated engine cycles that follow similar repeating patterns organized about the noisy period-2 fixed point. (Starting indices: 192, 403, 612, 910, 1236, 1338, 1476, 1959, 2261.)

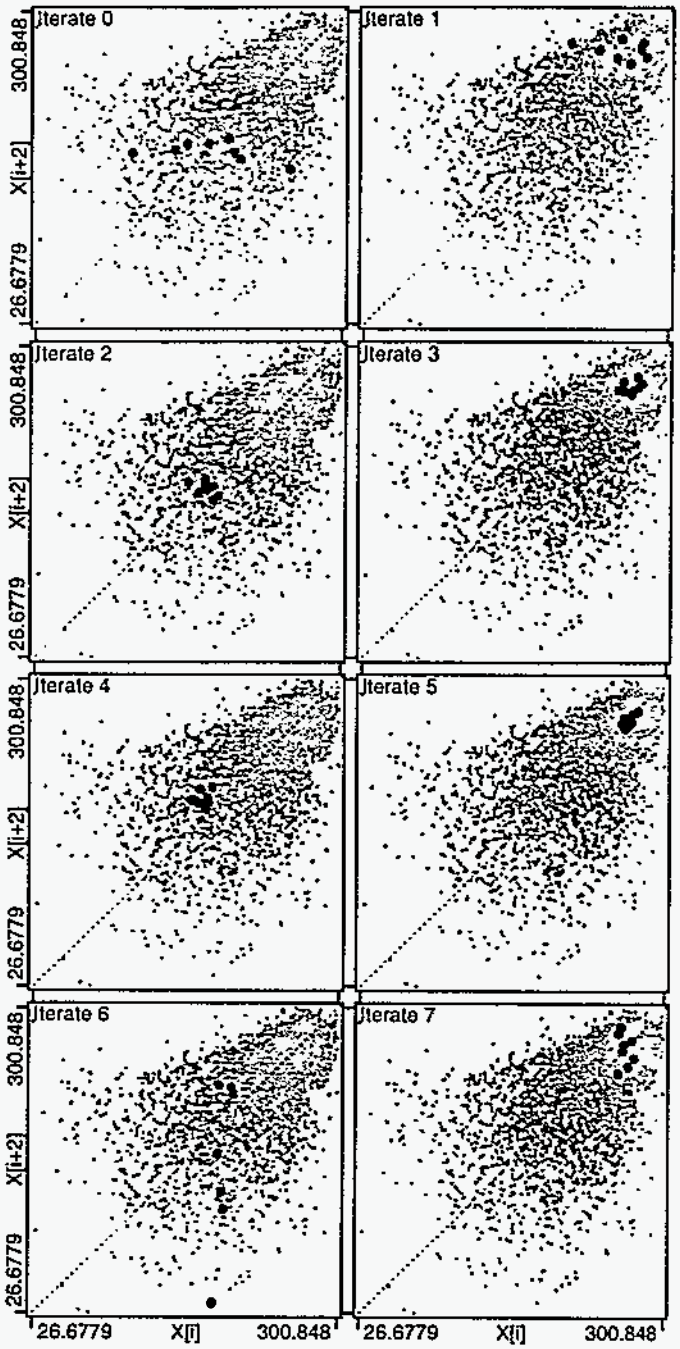

Figure 12: Experimental return map sequences for moderately lean fueling. Dark points represent uncorrelated engine cycles that follow similar repeating patterns organized about the noisy period-2 fixed point. (Starting indices: 217, 284, 357, 448, 857, 1047, 1523, 2440.)

unstructured cluster ("shotgun" pattern).

As shown in Fig. 9 and 10, the return maps for both the model and experiment follow a trend from a small "noisy" point to an extended "banana-shaped" pattern to a more complex extended shape with reducing equivalence ratio. This suggests that a similar pattern of instability develops in both cases.

We concentrate on more specific details in the instability patterns at moderately lean fueling in Fig. 11 and 12. Here the return-map axes have been modified to heat release in cycle i versus heat release in cycle $i+2$. These coordinates were selected because period-2 patterns are expected to appear as points on the diagonal. The light shaded points represent the map for all of the observations. The darker points are from a selected set of engine cycles that are tracked sequentially in time in the successive frames (iterate 0, iterate 1 and so on). Indices listed in the figure captions represent the beginning cycle numbers (for the frame marked "Iterate 0") of the dark points. The patterns followed by the dark points reveal defining characteristics of deterministic chaos. Specifically, we see clear evidence for period-2 fixed points and their associated stable and unstable manifolds. As shown, the darker points collapse together along the stable manifolds (linear point clusters with shallow slopes)

onto the fixed points, oscillate between the fixed points for several iterates, and then diverge from the fixed points (and each other) along unstable manifolds (linear point clusters with steep slopes). The occurrence of these patterns in both the model and experimental data implies similar dynamics. The chance of finding such patterns in random data is infinitesimally small.

CONCLUSIONS

The purpose of our model is to provide a physically reasonable hypothesis to explain the specific time-resolved *patterns* observed in cyclic variability. Other investigators have observed "prior-cycle" effects, specific observations concerning cycle-resolved time series measurements, but these have been typically presented in a strictly linear framework, concentrating on autocorrelation. Our model shows how such autocorrelation can arise but in a more "physics-oriented" presentation, making specific predictions about the structure of the time series, which is best resolved through nonlinear data analysis techniques. Such evidence is the observation of similar shapes in the return maps, and the presence of an underlying bifurcation to "noisy-period-2" behavior at lean fueling.

All parameter values that we have chosen are well within the range of physical plausibility, and we are currently engaged in producing an algorithm which can determine best fits from observed time series measurements. The model is specific enough that there is little chance that the similar trends and patterns produced by the model and experiment could be caused by overfitting an overly general and unrealistic mathematical function.

Chaotic data analysis confirms the presence of deterministic behavior with dynamical noise in the observed engine consistent with the model results. The ability of our model to exhibit both stochastically and deterministically dominated regimes may help explain apparent discrepancies in previous observations as cyclic variation has been observed to appear either as an independent stochastic process or one with deterministic prior-cycle effects. We have not addressed the question of whether "the engine dynamics are chaotic". However, we see, in model and experiment, dynamical behaviors that are typically associated with "deterministic chaos" but which we believe are distinct from classical deterministic chaos because of the existence and importance of the dynamical noise, herein modeled as random fluctuations in the parameters. This noise is not simply additive but is nonlinearly amplified by the physics of the combustion curve and the cyclic dynamics. The ability to describe engine fluctuations with such a simple yet physically plausible model may aid in the development of cycle-resolved control schemes to reduce or alter the pattern of cyclic fluctuations in order to improve efficiency or emissions.

ACKNOWLEDGEMENTS

This work is supported by the U.S. Department of Energy, Office of Energy Research and the Ford Motor Company.

REFERENCES

1. Clerk, D., **The Gas Engine**, 1st ed., Longmans, Green & Co., 1886.
2. Belmont, M.R., M.S. Hancock, and D.J. Buckingham, "Statistical aspects of cyclic variability", SAE Paper No. 860324, 1986.
3. Brehob, D.D. and C.E. Newman, "Monte Carlo simulation of cycle-by-cycle variability", SAE Paper No. 922165, 1992.
4. Daily, J.W., "Cycle-to-cycle variations: a chaotic process?", *Combustion Science and Technology* **57**, 149–162, 1988.
5. Grünefeld, G., V. Beushausen, P. Andresen, and W. Hentschel, "A major origin of cyclic energy conversion variations in SI engines: cycle-by-cycle variations of the equivalence ratio and residual gas of the initial charge", SAE Paper No. 941880, 1994.
6. Hamai, K., H. Kawajiri, T. Ishizuka, and M. Nakai, "Combustion fluctuation mechanism involving cycle-to-cycle spark-ignition variation due to flow motion in SI engines", *21st International Symposium on Combustion*, 505–512, 1986.
7. Hill, P.G. and A. Kapil, "The relationship between cyclic variation in spark-ignition engines and the small structure of turbulence", *Combustion and Flame* **78**, 237–247, 1989.
8. Kantor, J.C., "A dynamical instability of spark-ignited engines", *Science* **224**, 1233–1235, 1984.
9. Kumar, S., M.D. De-Zylva, and H.C. Watson, "Prediction of cyclically-variable pressure-time history of a SI engine using a quasi-dimensional spherical flame-front model", SAE Paper No. 912454, 1991.
10. Martin, J.K., S.L. Plee, and D.J. Remboski, Jr., "Burn modes and prior-cycle effects on cyclic variations in lean-burn spark-ignition engine combustion", SAE Paper No. 880201, 1988.
11. Moriyoshi, Y., T. Kanimoto, and M. Yagita, "Prediction of cycle-to-cycle variation of in-cylinder flow in a motored engine", SAE Paper No. 930066, 1993.
12. Ozdor, N., M. Dulger, and E. Sher, "Cyclic variability in spark-ignition engines: a literature survey", SAE Paper No. 940987, 1994.
13. Glassman, I. **Combustion**, 2nd ed., Academic Press, ISBN 0-12-285851-4, 1987.
14. Heywood, J.B. **Internal Combustion Engine Fundamentals**, McGraw-Hill, ISBN 0-07-028637-X, 1988.
15. Takens, F. "Detecting strange attractors in turbulence", in *Lecture Notes in Mathematics* **898**, 366–381, 1981.
16. Moon, F.C., **Chaotic and Fractal Dynamics**, John Wiley and Sons, ISBN 0-471-54571-6, 1992.

NOMENCLATURE

$C[n]$	Dimensionless combustion efficiency curve, a function of $\Phi[n]$
C_{max}	Maximum combustion efficiency, achieved at stoichiometric fueling
F	Actual fraction of unreacted gas and fuel remaining from previous cycle
F_o	Nominal fraction of unreacted gas and fuel remaining in the cylinder
$m[n], a[n]$	Actual masses of fuel and air before the nth combustion event, including residual and new
$m_{new}[n], a_{new}[n]$	New mass of fuel and air procured from the intake manifold on the nth event
$m_{res}[n], a_{res}[n]$	Residual mass of fuel and air before the nth combustion event
m_o, a_o	Reference masses of fuel and air fed to cylinder when no residual gas present, used to nondimensionalize dynamical system
$N(0,1)$	Gaussian random number with mean zero and standard deviation one
w_f, w_a	Molecular weights of fuel and air
$Q[n]$	Proportional to the heat released on the nth cycle, the principal observed time series
R	Mass ratio of air to fuel at stoichiometric conditions.
$\Phi[n]$	In-cylinder instantaneous fuel-air equivalence ratio before spark
ϕ_o	Nominal as-fed equivalence ratio
ϕ_l, ϕ_u	Lower 10 and upper 90 percent locations of the combustion-efficiency function
ϕ_m	Midpoint between ϕ_l and ϕ_u
Σ	Dimensionless ratio of molecular weight of fuel to air
σ_F	Standard deviation of the fluctuations in F
σ_ϕ	Standard deviation of the noise perturbing ϕ
*	When used as a superscript, designates a dimensionless quantity

DISCLAIMER

This report was prepared as an account of work sponsored by an agency of the United States Government. Neither the United States Government nor any agency thereof, nor any of their employees, makes any warranty, express or implied, or assumes any legal liability or responsibility for the accuracy, completeness, or usefulness of any information, apparatus, product, or process disclosed, or represents that its use would not infringe privately owned rights. Reference herein to any specific commercial product, process, or service by trade name, trademark, manufacturer, or otherwise does not necessarily constitute or imply its endorsement, recommendation, or favoring by the United States Government or any agency thereof. The views and opinions of authors expressed herein do not necessarily state or reflect those of the United States Government or any agency thereof.